Acta Mechanica Slovaca **29 (2): 26 - 31,** June **2025**
https://doi.org/10.21496/ams.2025.016

Acta Mechanica Slovaca
ISSN 1335-2393
www.actamechanica.sk

Enhancing Residual Stress Mitigation in SLM-Fabricated Ti6Al4V Through Process Parameter Optimization and Remelting Techniques

Marek Gazda [1], Jiří Hajnyš [1,*], Akash Nag [1], Jana Petrů [1], Quoc-Phu Ma [1]

[1] Department of Machining, Assembly and Engineering Technology, Faculty of Mechanical Engineering, VSB-TU Ostrava, 17. Listopadu 2172/15, 70800 Ostrava, Czech Republic

Abstract: This study investigates the reduction of residual stresses in Ti6Al4V parts produced via Selective Laser Melting (SLM) by optimizing process parameters and incorporating remelting techniques. The effects of laser power, scanning speed, hatch distance, and remelting cycles were analysed using bridge-shaped samples and deformation angle measurements. The Design of Experiment (DoE) study with Taguchi method was utilized to optimize the number of parameter combinations, effectively reducing the number of required experiments. In addition, a modified Volumetric Energy Density (VED) formula accounting for remelting cycles was proposed to provide deeper insights into energy distribution and stress formation in the printed sample. Results indicate that higher laser power and multiple remelting cycles significantly reduce residual stress, but their effects are less stable, evident from the significant variation among the measured results. Meanwhile, scanning speed and hatch distance had minimal effects on the residual stress. According to the DoE study, the best parameter set for minimal residual stress - in order of laser power, scanning speed, hatch distance, and remelting cycles - is (200 W, 1000 mm/s, 0.05 mm, 5 remelting cycles).

Keywords: SLM; Residual stress; Process parameters, Remelting, VED, Taguchi method.

1. Introduction

Selective Laser Melting (SLM), a process that utilizes metallic materials such as steel alloys, aluminium, nickel, and titanium, among others, is gaining popularity in Additive Manufacturing (AM) [1]. Among the most widely used materials to be printed is titanium alloy Ti6Al4V. Owing to its exceptional corrosion resistance, strength-to-weight ratio, and biocompatibility, it is well-suited for applications in the aerospace and medical domains [2]. Moreover, SLM enables the fabrication of highly complex geometries from this otherwise difficult-to-machine material, underscoring its importance for further research.

In order to manufacture a component with SLM technology, it is necessary to create an electronic model of the component in Computer-aided design (CAD) software and export it in Stereolithography (STL) format. The model is subsequently exported into a slicer to prepare printing programs of the part for the printer. Since SLM technology utilizes a laser to melt metal powder layer-by-layer to create the finished part, it is essential to establish process parameters related to the laser and how the powder is layered, because that significantly affects the mechanical properties of the printed part [3-5]. The crucial parameters include laser power, scanning speed, hatch distance, and layer height [4]. By measuring these values, we can calculate the Volumetric Energy Density (VED), a critical metric for assessing the energy content of the material printed

*** Corresponding author:** Jiří Hajnyš, ***E-mail address:*** *jiri.hajnys@vsb.cz*

using SLM technology [6].

The remelting process is an additional and crucial parameter in SLM. Instead of melting a layer only once, we can remelt it multiple times. This approach has the potential to enhance various mechanical properties, such as reducing porosity and residual stress [7]. In SLM, when the laser melts a layer of metallic powder, it forms a melt pool. The heat emanated from this pool affects not only the layer being printed but also penetrates into the previous layers causing rapid and repeated heating and cooling cycles [8]. This results in a remarkably complex thermal history, leading to the complex residual stress development within the printed component. During printing, the thermal distribution in the z-direction can be categorized into three distinct regions: the melted zone (region I), the heat-affected zone (region II), and the non-affected zone (region III) [9]. Introducing remelting process (melting on a layer multiple times) significantly influences the melt pool dynamics and increases the total energy input to the printed component. However, this effect is not accounted for in the conventional VED formula [10–12], highlighting the need to modify the original VED formulation in this study.

Here, Ti6Al4V samples were fabricated using SLM technology. The investigation examined the effects of laser power, scanning speed, hatch distance, and the remelting process on residual stress formation. Bridge-shaped samples were selected for residual stress quantification. Specifically, a bridge will deform an angle once it is successfully printed and removed from the substrate, owing to the residual stress relaxation. The higher the residual stress inside the part, the higher the deformed angle. The measured angles were then subjected to statistical analysis using DoE to identify the parameters exerting the greatest influence on residual stress. The objective of this work is to mitigate residual stress through the optimization of process parameters and the application of remelting.

2. Experimental Section

As aforementioned, the objective of the study was to ascertain the influence of process parameters and remelting processes on residual stress in SLM technology. The bridge samples were fabricated, cut from the substrate and measured to analyse the angle of each sample. After fabrication, the samples were cut from the substrate so that we could measure their angle The printing parameters employed in this study is presented in Table 1. The parameters selected for investigation include laser power (P), scanning speed (v), hatch distance (hs), and the number of remelting processes (n). These parameters will be examined to determine their impact on residual stress within the experimental framework because they are the most influential [13-15].

Table 1: Chosen process parameters.

P (W)	v (mm/s)	hs (mm)	n (-)
200	500	0.05	1
250	750	0.1	3
300	1000	0.2	5

2.1 Design of the sample

The sample employed in this study is a bridge with dimensions of 30 x 18 x 15 mm^3 (Fig 1). It is important to note that all samples possess an identical layer thickness, which is set at 60 µm. This value is chosen for the balance between printing quality and build time. Moreover, the chessboard scanning strategy is used. The Taguchi method (details in Table 2) was used in this experiment for its time and cost efficiency instead of Full Factorial design. It enables the examination of multiple variables using orthogonal arrays with minimal experiments. Additionally, the utilization of bridge samples facilitates the acquisition of data with minimal effort through the measurement of virtually any CAD model. Herein, SolidWorks (ver. 2022) was employed following prior study [4].

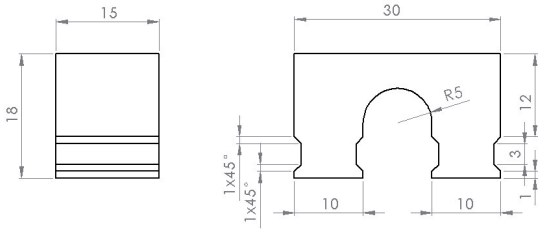

Figure 1: Bridge sample (mm).

Table 2: Taguchi method.

Number of parameters	4
Number of levels	3
Taguchi Array	L9(3^4)
Combination of parameters	9

2.2 Fabrication

The fabrication process involved the utilization of a 3D printer manufactured by British company Renishaw plc, specifically the metallic 3D printer RenAM 400 model. RenAM 400 is equipped with a build plate measuring 250 x 250 x 300 mm^3, a laser with maximum power of 400 W, and layer thickness ranging from 20 µm to 100 µm. After printing, we take our substrate and cut our samples from the substrate using the WEDM Fanuc Robocut α-C400iC machine with precision of 0.1 mm to 0.3 mm. For this experiment, the titanium alloy Ti6Al4V was utilized. The material properties and its composition are shown in Table 3 and Table 4 [16].

Table 3: Mechanical properties of Ti–6Al–4V at room temperature [17].

Condition	Microcrystalline
Yield stress	960 MPa
Ultimate tensile strength	1050 MPa
Area reduction	32 %
Total elongation	9 %
Uniform elongation	0.9 %
Fatigue limit	580 MPa

Table 4: Material composition of Ti6Al4V [16].

Ti (%)	Al (%)	V (%)	Fe (%)
88.93	6.4	4.1	0.18

2.3 Measurement

The Alicona Infinite Focus G5 is the instrument of choice for measurement. This microscope is characterized by its exceptional precision, with an accuracy of up to 10 nm. It functions based on focus variation, which involves focusing an image at multiple levels, thereby producing an image of superior quality [18].

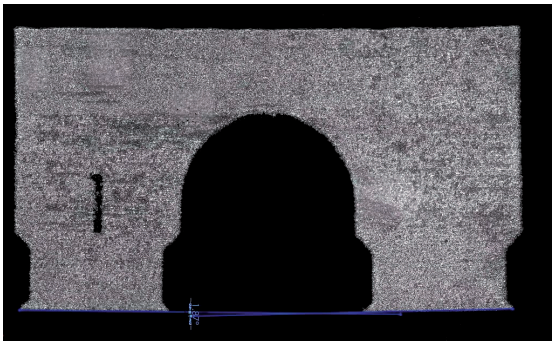

Figure 2: Angle measurement of the bridge sample (mm).

Subsequently, the process of measurement is executed using the SolidWorks software. This is achieved through taking images of the bridges from Alicona and setting of two lines under the pillars of the sample. The final step entails measuring the angle formed by these two lines in the CAD software SolidWorks as can be seen in Fig 2.

3. Results and Discussion

Traditionally, the VED values are calculated using the formula shown below in Equation 1, which incorporates the most influential printing parameters affecting residual stress formation [19].

$$E_v = \frac{P}{v \cdot hs \cdot t} \quad (1)$$

The remelting process used in our experiment requires us to include this phenomenon in the formula for a more accurate calculation of the VED (Equation 2). The VED formula is generally applied when a single layer is scanned as it indicates the total amount of energy (J) that is put inside one mm3 volume of the printed material. By remelting n times the layers, we introduce n times the energy input to the same volume of material. For that, to incorporate this effect, we change the formula of VED as follows.

$$E_v = \frac{P}{v \cdot hs \cdot t} \cdot n \quad (2)$$

With the inclusion of n into the VED formula, the distribution of angle versus the new VED can be plotted in Figure 3. In addition, the resulting angles of the bridges and corresponding printing parameters are reported in Table 5.

Table 5: Results.

P (W)	v (mm/s)	hs (mm)	n (-)	VED (J/mm^3)	Angle (°)
250	750	0.2	1	27.8	2.57± 0.08
300	1000	0.1	1	50	2.41±0.08
200	1000	0.2	5	83.3	1.86±0.30
200	500	0.05	1	133.3	1.94±0.14
200	750	0.1	3	133.3	2.32±0.51
300	500	0.2	3	150	2.93±0.10
250	1000	0.05	3	250	2.6±0.16
250	500	0.1	5	416.7	2.33±0.37
300	750	0.05	5	666.7	2.13±0.30

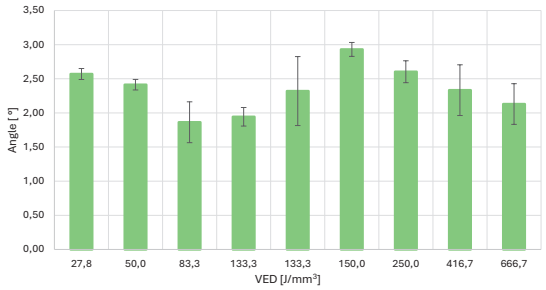

Figure 3: Relationship between angle and new VED.

New data with recalculated VED was put into Minitab (ver. 2022), where we applied Taguchi analysis to analyze the effect plot of the mean and the signal to noise ratio. Within the framework of our analysis, we adopted the smaller is better approach because the smallest angle as possible is desired. The main effects plot for means are presented in Figure 4 and Table 6, while those for the signal-to-noise ratio (S/N ratio) are shown in Figure 5 and Table 7.

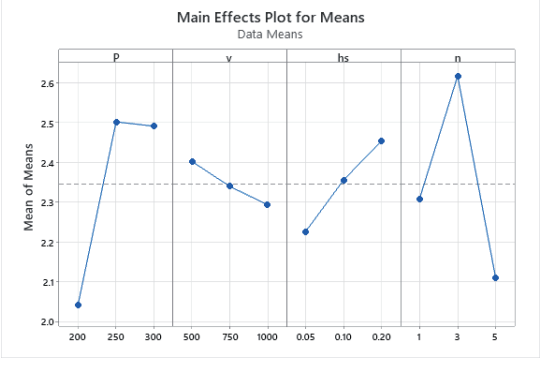

Figure 4: Main effects plot for Means.

Table 6: Response Table for Means.

Level	P (W)	v (mm/s)	hs (mm)	n (-)
1	2.04	2.4	2.23	2.31
2	2.5	2.34	2.36	2.62
3	2.49	2.29	2.45	2.11
Delta	0.46	0.11	0.23	0.51
Rank	2	4	3	1

As can be observed in Fig. 4, the results indicate an almost linear relationship between the angle and the scanning speed as well as the hatch distance. Specifically, higher scanning speed corresponds to lower angle, while higher hatch distance corresponds to higher angle. However, the relationship between laser power and the remelting process is more complex. For laser power, 200 W appears to have the lowest average angle, and the lowest dispersion (as can be observed together with S/N ratio plot in Fig 5.). On the other hand, 250 W has the highest average angle, and the highest dispersion. A similar outcome is observed in the remelting process, where five remelting processes yield the lowest average angle, and lowest dispersion, while three remelting processes result in the highest average angle, and highest dispersion. Tables 6 and 7 also show that the most influential parameter on the angle (residual stress) is remelting time, followed by laser power, hatch distance, and scanning speed.

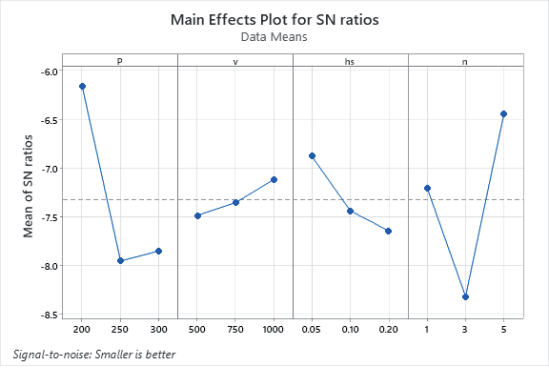

Figure 5: Main effect plot for SN ratios.

Table 7: Response Table for Signal to Noise Ratios (Smaller is better).

Level	P (W)	v (mm/s)	hs (mm)	n (-)
1	-6.162	-7.489	-6.883	-7.207
2	-7.956	-7.359	-7.441	-8.319
3	-7.852	-7.123	-7.647	-6.444
Delta	1.794	0.366	0.764	1.875
Rank	2	4	3	1

In the final stage of our statistical analysis, we employed a correlation approach to ascertain the relationship between each parameter. The outcomes of these correlation analyses substantiate our initial assertions concerning the behaviour of the four parameters as can be seen in Table 8.

The correlation analysis reconfirms the effect plots presented in Fig 4. and Fig 5. It shows that laser power has the strongest influence on the deformation angle (0.58), indicating that higher power increases residual stress. Meanwhile, hatch distance has a weaker positive effect (0.29), meaning larger spacing slightly increases

Table 8: Correlations.

	P (W)	v (mm/s)	hs (mm)	n (-)	Angle (°)	VED (J/mm³)	Deviation (mm)	SNRA1 (-)
v	0	-	-	-	-	-	-	-
hs	0	0	-	-	-	-	-	-
n	0	0	0	-	-	-	-	-
Results	0.58	-0.14	0.29	-0.26	-	-	-	-
VED	0.36	-0.22	-0.53	0.67	-0.15	-	-	-
Deviation	-0.45	-0.07	-0.19	0.65	-0.39	0.38	-	-
SNRA1	-0.58	0.13	-0.25	0.26	-0.1	0.13	0.36	-
MEAN1	0.58	-0.14	0.29	-0.26	1	-0.15	-0.39	-0.1

the angle. In contrast, the remelting parameter exhibits a moderate negative correlation (-0.26), suggesting that additional remelting reduces angle. Additionally, scanning speed shows only a weak negative correlation (-0.14). Last but not least, VED has a weak negative correlation (-0.15), suggesting it alone cannot fully capture residual stress behaviour, particularly when remelting is considered. Overall, laser power, hatch distance, and remelting emerge as the most significant factors affecting residual stress, while scanning speed, and VED play secondary roles. The identification of optimal parameters is facilitated by the Minitab function "Predicted values," which is instrumental in this regard (Table 9).

Table 9: Parameters with lowest and highest average residual stress value.

Ranking	P (W)	v (mm/s)	hs (mm)	n (-)
Lowest	200	1000	0.05	5
Highest	250	500	0.2	3

The first combination of parameters (200 W, 1000 mm/s, 0.05 mm, 5 remelting cycles) resulted in the lowest average residual stress in terms of angle. In addition, it is the most stable due to the previous S/N ratio assessment. In contrary, the worst combination of parameters that yields the highest average angle (250 W, 500 mm/s, 0.2 mm, 3 remelting cycles) is also the most unstable.

4. Conclusions

This paper aimed to identify optimal process parameters for reducing residual stress in the remelting of Ti6Al4V using SLM technology. Four key parameters¬, that is, laser power, scanning speed, hatch distance, and the remelting process, were examined at three levels each. The Taguchi method, implemented in Minitab, was employed to analyse nine parameter combinations, each combination is repeated three times, resulting in 27 samples in total. Residual stress was evaluated by observing bridge deformation, with the angle between deformed pillars measured after precise cutting of samples. Bridges were designed in SolidWorks, process parameters configured in the Material Editor, and g-code generated using QuantAM for 3D printing. Samples were cut with by WEDM machine and measured. The data analysis included calculating means, deviations, and the S/N ratio to evaluate the influence of parameters on residual stress.

Results showed that the remelting process and laser power had a significant impact on reducing residual stress compared to other parameters. A linear relationship was observed between hatch distance and scanning speed, while a more complex interaction occurred between laser power and remelting. No strong correlation was found between VED and residual stress. These findings demonstrate the importance of precise parameter manipulation and remelting in influencing residual stress. The microstructural analysis was not considered into the scope of this experiment. However, it is important to acknowledge the significance of microstructural analysis in the future research.

Based on the DoE study, the optimal parameter set for minimal residual stress in terms of both average value and stability is (200 W, 1000 mm, 0.05 mm/s, 5 remelting cycles). It is hoped that the present work will serve as a catalyst for further research in this area. In addition, the study highlighted residual stress as a complex phenomenon and validated the bridge sample method as efficient and comprehensible. Adjustments to the VED formula incorporating remelting require further validation. Exploring the

impact of remelting on additional properties, such as porosity and ductility, could further enhance understanding.

Acknowledgments

This paper has been done in connection with project Students Grant Competition SP2025/062 „Specific research on progressive and sustainable production technologies" and SP2025/063 „Specific research on innovative and progressive manufacturing technologies" financed by the Ministry of Education, Youth and Sports and Faculty of Mechanical Engineering VŠB-TUO.

References

[1] J. Mesicek et al., "Abrasive surface finishing on slm 316l parts fabricated with recycled powder," Applied Sciences (Switzerland), vol. 11, no. 6, Mar. 2021, doi: 10.3390/app11062869.

[2] L. C. Zhang and H. Attar, "Selective Laser Melting of Titanium Alloys and Titanium Matrix Composites for Biomedical Applications: A Review," Apr. 01, 2016, Wiley-VCH Verlag. doi: 10.1002/adem.201500419.

[3] P. Snopiński, K. Matus, O. Hilšer, and S. Rusz, "Effects of Built Direction and Deformation Temperature on the Grain Refinement of 3D Printed AlSi10Mg Alloy Processed by Equal Channel Angular Pressing (ECAP)," Materials, vol. 16, no. 12, Jun. 2023, doi: 10.3390/ma16124288.

[4] J. Hajnys, M. Pagáč, J. Měsíček, J. Petru, and M. Król, "Influence of scanning strategy parameters on residual stress in the SLM process according to the bridge curvature method for AISI 316L stainless steel," Materials, vol. 13, no. 7, Apr. 2020, doi: 10.3390/ma13071659.

[5] P. Snopiński, A. N. S. Appiah, O. Hilšer, and M. Kotoul, "Investigation of Microstructure and Mechanical Properties of SLM-Fabricated AlSi10Mg Al-loy Post-Processed Using Equal Channel Angular Pressing (ECAP)," Materi-als, vol. 15, no. 22, Nov. 2022, doi: 10.3390/ma15227940.

[6] M. A. Buhairi et al., "Review on volumetric energy density: influence on morphology and mechanical properties of Ti6Al4V manufactured via laser powder bed fusion," Apr. 01, 2023, Springer Science and Business Media Deutschland GmbH. doi: 10.1007/s40964-022-00328-0.

[7] E. Yasa and J. Kruth, "APPLICATION OF LASER RE-MELTING ON SELECTIVE LASER MELTING PARTS," Advances in Production Engineering & Management, vol. 6, pp. 259–270, 2011.

[8] B. He, C. Bi, X. Li, W. Wang, and G. Yang, "Residual stresses and deformations of laser additive manufactured metal parts: a review," Jan. 01, 2023, Springer-Verlag Italia s.r.l. doi: 10.1007/s12289-022-01729-w.

[9] Y. Liu, Y. Yang, and D. Wang, "A study on the residual stress during selective laser melting (SLM) of metallic powder," International Journal of Advanced Manufacturing Technology, vol. 87, no. 1–4, pp. 647–656, Oct. 2016, doi: 10.1007/s00170-016-8466-y.

[10] S. Pal et al., "Mechanisms of defect formation in Ti-6Al-4V product during re-melting of layers in selective laser melting," J Manuf Process, vol. 105, pp. 260–275, Nov. 2023, doi: 10.1016/j.jmapro.2023.09.044.

[11] M. Zhao, C. Duan, and X. Luo, "Heat Transfer, Laser Remelting/Premelting Behavior and Metallurgical Bonding During Selective Laser Melting of Metal Powder," Metals and Materials International, vol. 28, no. 9, pp. 2225–2238, Sep. 2022, doi: 10.1007/s12540-021-01129-w.

[12] A. Paraschiv, G. Matache, N. Constantin, and M. Vladut, "Investigation of Scanning Strategies and Laser Remelting Effects on Top Surface Deformation of Additively Manufactured IN 625," Materials, vol. 15, no. 9, May 2022, doi: 10.3390/ma15093198.

[13] T. Mishurova et al., "An assessment of subsurface residual stress analysis in SLM Ti-6Al-4V," Materials, vol. 10, no. 4, Mar. 2017, doi: 10.3390/ma10040348.

[14] Z. Wang, Z. Xiao, Y. Tse, C. Huang, and W. Zhang, "Optimization of pro-cessing parameters and establishment of a relationship between microstructure and mechanical properties of SLM titanium alloy," Opt Laser Technol, vol. 112, pp. 159–167, Apr. 2019, doi: 10.1016/j.optlastec.2018.11.014.

[15] Z. Xiao et al., "Study of residual stress in selective laser melting of Ti6Al4V," Mater Des, vol. 193, Aug. 2020, doi: 10.1016/j.matdes.2020.108846.

[16] M. G. Scaramuccia, A. G. Demir, L. Caprio, O. Tassa, and B. Previtali, "Development of processing strategies for multigraded selective laser melting of Ti6Al4V and IN718," Powder Technol, vol. 367, pp. 376–389, May 2020, doi: 10.1016/j.powtec.2020.04.010.

[17] S. Zherebtsov, G. Salishchev, R. Galeyev, and K. Maekawa, "Mechanical Properties of Ti-6Al-4V Titanium Alloy with Submicrocrystalline Structure Produced by Severe Plastic Deformation."

[18] J. Galík, D. Varecha, M. Drbúl, R. Madaj, and V. Konstantová, "Design and optimization of the construction of a mobile disinfection chamber for small communication devices and small objects," Production Engineering Archives, vol. 29, no. 2, pp. 201–215, Jun. 2023, doi: 10.30657/pea.2023.29.24.

[19] E. M. Pechlivani, L. Melidis, S. Pemas, K. Katakalos, D. Tzovaras, and A. A. Konstantinidis, "On the Effect of Volumetric Energy Density on the Characteristics of 3D-Printed Metals and Alloys," Metals (Basel), vol. 13, no. 10, Oct. 2023, doi: 10.3390/met13101776.